World Applied Sciences Journal 32 (5): 780-791, 2014
ISSN 1818-4952

DOI: 10.5829/idosi.wasj.2014.32.05.14532

Punching Shear Strength of Pre-Stressed Flat Slab in Case of Near-Column Openings

Hesham Eid, Kaled. H. Riad and Amr H. Zaher

Department of Structural Engineering,
Faculty of Engineering, Ain Shams University, Cairo, Egypt

Abstract: The paper focuses on the effect of openings on punching shear strength of post-tensioned flat slabs supported on square columns. Five slab specimens had been tested under concentrated load and it was found, that the openings reduce punching strength considerably. The accuracy of the strut-and-tie model together with the design equations of ACI, CSA, ECP, BS and CEBcodes of practice has been. For the prediction of the punching shear strength of the tested specimens and for evaluating the effect of the near column openings, the strut-and-tie model proposed by Emad Raouf, 2010 for calculating the punching shear strength of non-pre-stressed slabs are used. In addition, proposed methods for calculating the punching shear strength of post-tensioned slabs using modified ECP equation are introduced and evaluated using the present experimental results in addition to 40 experimental results from the literature. The proposed strut-and-tie model is found to be accurate.

Key words: Near-column opening · Pre-stressed flat slabs · Punching shear strength · Strut-and -tie model.

INTRODUCTION

In recent years, the post-tensioned flat slabs system has been increasingly adopted for high-rise residential buildings all over the world. A typical modern residential building would have an irregular column layout. A large opening may also be present next to the column. Present recommendations for estimating the punching resistance of post-tensioned slabs at internal connections are basically empirical and there are considerable differences between them. Experimental data on post-tensioned slabs with openings and supported on square columns are also very limited. For this reason, research has been initiated at Ain Shams University (ASU)-Egypt for the purpose of finding a practical solution for the structural design of this type of post-tensioned flat slab floor. This paper focuses on the effect of openings located near the column on the punching shear strength of post-tensioned flat slabs supported on square columns. The main variable is opening size and location. The paper presents tests to failure of five slabs; three are post-tensioned and two are non-prestressed slabs with different opening sizes and locations. The slabs did not have any shear reinforcement and were subjected to concentric punching. The parameters included in the investigation are the size and location of opening located near the column and the effect of prestressing. The test results were compared with the ACI [1], CSA [2], ECP [3], BS [4] and CEB [5] equations. In addition, the strut-and-tie model proposed by Rizk [6] for calculating the punching shear strength of non-prestressed slabs is used to calculate the punching shear strength of the tested post-tensioned slabs. The comparison between the experimental results and the predictions shows that the proposed strut-and-tie model is relatively more accurate than the current ACI[1], CSA[2], ECP[3], BS[4] and CEB[5] equations. Proposed modified method is introduced to enhance the punching shear strength predictions in ECP[3] code and evaluated using the present experimental results in addition to 40 experimental results from the literature.

Research Significance: The results of the tests reported herein and those collected from the literature provide a basis for assessing the reliability of different methods of designing for punching shear in post-tensioned slabs. The comparison made with five international codes clarify the present situation and point out some possibilities for improvements. In addition, a strut-and-tie model for calculating the punching strength of post-tensioned slabs

Corresponding Author: Amr H. Zaher, Structural Engineering Department, Faculty of Engineering, Ain Shams University, Cairo, Egypt.

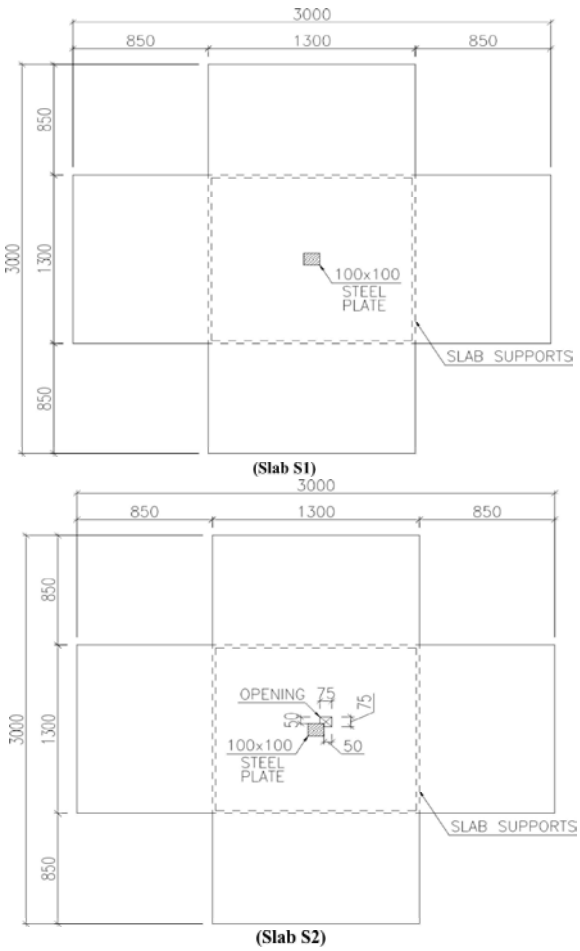

Fig. 1(a) : Plan for tested slabs S1 and S2.

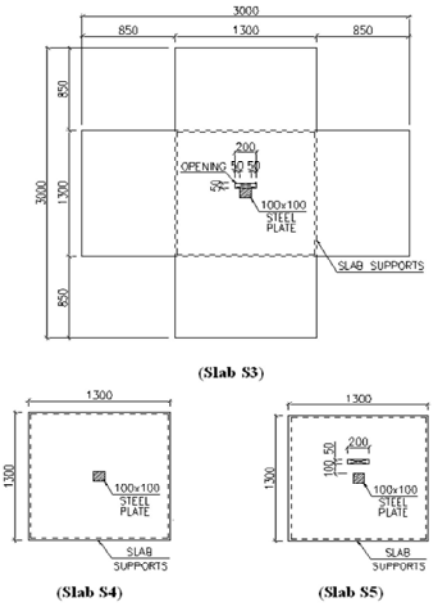

Fig. (1b): Plan for tested slabs S3, S4 and S5.

Table 1: Slabs perimeter length and crack and failure loads.

Slab ID	f_{cu}(N/mm^2)	b_o(mm)	0(N/mm^2)	V_{cr}(kN)	V_u(kN)
S1	37.6	721	2.03	175	260
S2	37.0	591	2.01	160	220
S3	37.0	461	1.65	140	170
S4	44.3	776	-	90	250
S5	44.3	647	-	60	180

Where bo is the effective perimeter calculated at distance 0.5d

is used and verified adequately. The authors hope that this research will be useful to design engineers and researchers dealing with the effect of openings on punching shear strength of post-tensioned flat slabs.

Test Program: Specimen Notations: Fig. 1 shows typical details of the five slab specimens. the overall slab thickness is 120 mm. grade 40 concrete was used. 0.6-inch diameter 7-wire mono-strands were used as post-tensioning tendons. the deformed steel bars had yield strength of 360 n/mm^2. Table 1 shows the material properties for each specimen. The column was represented as a square steel plate with 100 mm side dimension. flexural non-prestressed reinforcement of the test specimens consisted of 12 mm bars every 100 mm of high tensile steel bars provided at the bottom mesh and 8 mm every 200 mm at the top mesh reinforcement (Fig. 2). The reinforcement ratio provided was set higher than the normal value to ensure clear punching shear failure. thus, the effect of opening on punching shear strength can be observed clearly, with minimum interference from flexure. The layout of prestressing strands is shown in Fig. 3 to reduce the prestress loss due to anchorage draw-in of the short-length tendons, the lengths of post-tensioned specimens (S1, S2 and S3) were increased more than the non-prestressed specimens by 0.85m from each side.

Test Procedure: The specimens were subjected to an incremental static load till failure. During loading, all measurements, such as slab deflections, strains in internal non-prestressing steel bars and strain in the concrete were recorded at each increment. The load was applied in 10 kN to 20 kN increments. At each load increment, the cracking pattern was inspected and marked. The time required to load the slab to failure was usually between two and three hours. Fig. 4 shows a schematic diagram of the experimental setup, whereas a photo showing the slab being tested is shown in Fig. 5.

Serviceability Behavior: Under loading, the first cracks occurred at a load range of about 75% of the ultimate punching capacity for the post-tensioned slabs and 35%

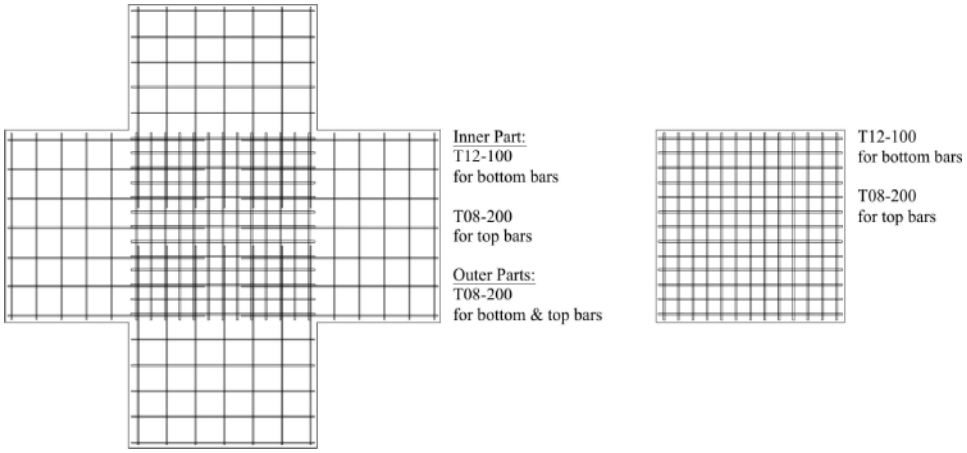

Fig. 2: Non-prestressing reinforcement details for tested post-tensioned slabs and non-prestressed slabs.

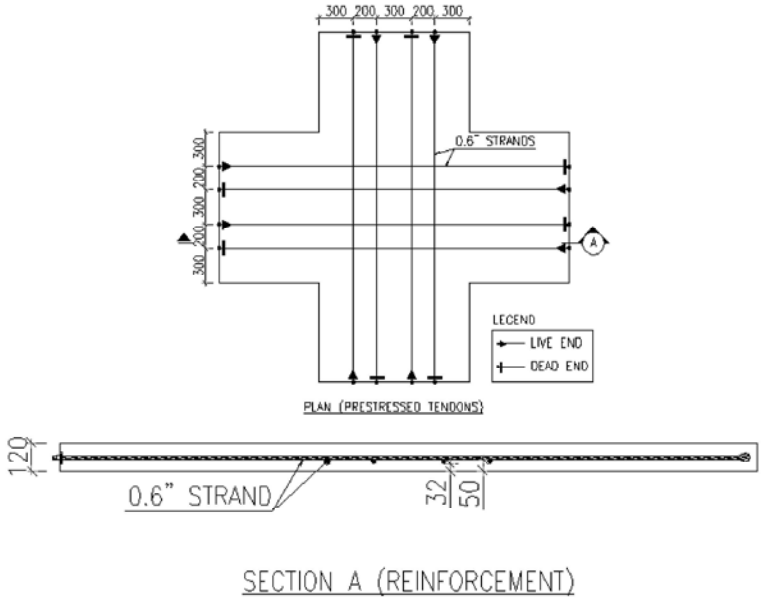

Fig. 3: Prestressing reinforcement plan and section for tested post-tensioned slabs.

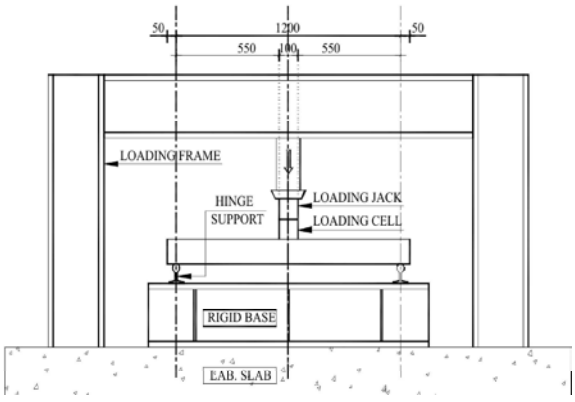

Fig. 4: Schematic test setup.

Fig. 5: Specimen S4 before testing.

Fig. 6: Failure of slab S1.

Fig. 7: Failure of slab S2.

Fig. 8: Failure of slab S3.

Fig. 9: Failure of slab S4.

Fig. 10: Failure of slab S5.

of the ultimate punching capacity for the non-prestressed slabs. The cracks started with longitudinal cracks running from the column stub toward the slab edges. This was shortly followed by the formation of circumferential cracks around the column stub. As the load was increased, circumferential cracks occurred at a location farther away from the column stub. Numerous cracks developed on the tension face of the slab at the time of failure. Figures 6 to 10 show the crack patterns for the five slab specimens after failure. In most cases, the major inclined shear cracks previously mentioned would become the final cracks that lead to the punching failures of the slabs. It was observed that for non-prestressed slabs failure punching shear crack had an inclination angle equal to 26°, but for post-tensioned slabs the inclination angle was equal to 32°.

Deflections: Fig. 11 shows the load-deflection curves at the center point of each specimen for the tested slabs. The opening reduces slab stiffness and leads to a greater deflection of the slab area near the opening. The linear behaviour at early stages of loading to failure load, for all slabs, proofs the brittle manner in which the slabs failed. The reduction in slope of load-deflection curves for slabs with opening after first crack is an indication that as the size of opening increased, the slab stiffness reduced and its ability to resist the load decreased.

Steel Strains: Measurements were made to determine the strain values of non-prestressed bottom reinforcement for all the test slabs at all stages of loading. The strain gauges were installed on the bottom bar next to the column face in each direction. Test results of these measurements are presented in Fig. 12. All post-tensioned slabs S1, S2 and S3 failed in punching shear before the yielding of non-prestressing steel took place.

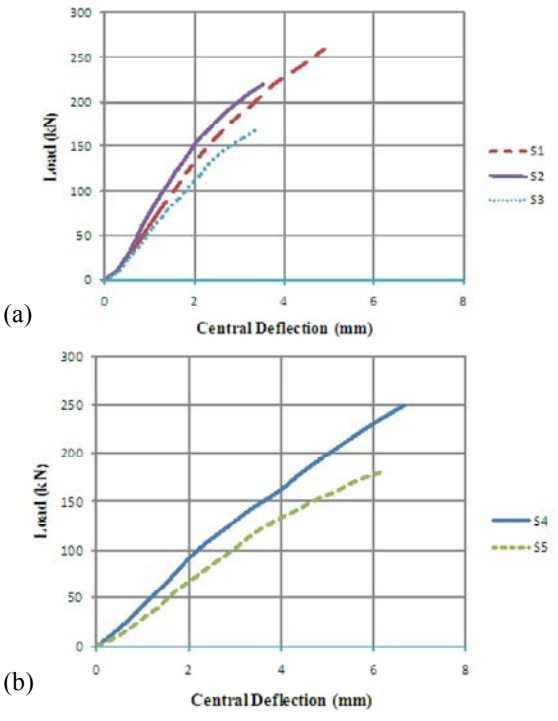

Fig. 11(a): Load-Deflection curves for S1, S2 and S3; and (b) Load-Deflection curves for S4 and S5

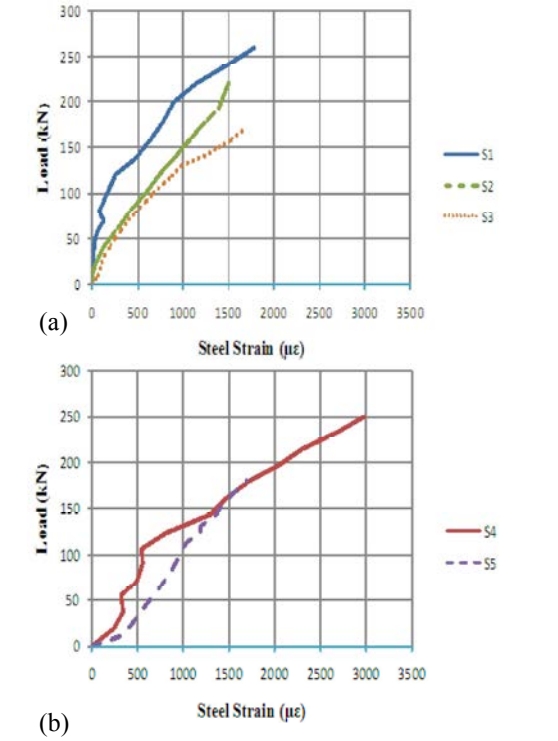

Fig. 12(a): Steel strain of slabs S1, S2 and S3; and (b) Steel strain of slabs S4 and S5.

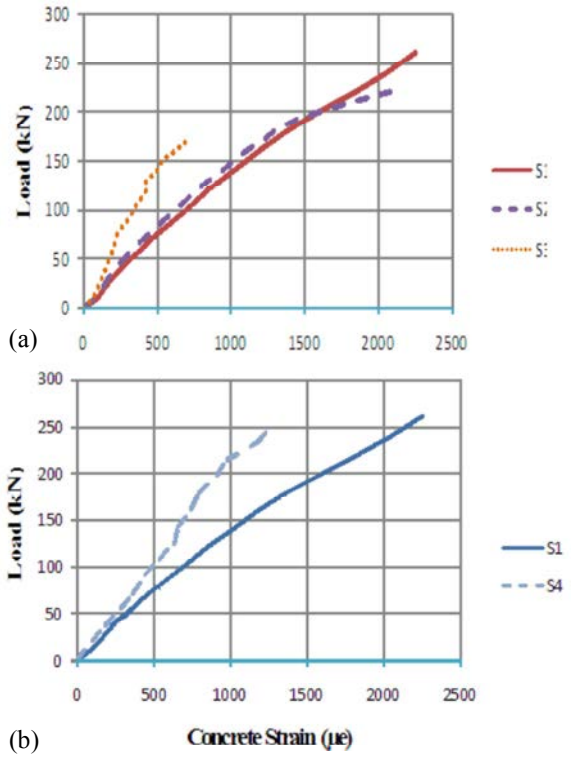

Fig. 13: Concrete strain of slabs (a) S1, S2 and S3; and (b) slabs S1 and S4.

The presence of the prestressing strands in post-tensioned slabs decreased the tension stress at the bottom of slabs and decreased the stresses on the tension steel. It is shown from the curves that as the opening size increased the strain in non-prestressing steel increased. For non-prestressed slabs S4 and S5, before cracking, the increase in steel strain was linear and relatively low up to the first visible cracking load.

Concrete Strains: Measurements were made to determine the strain value of the concrete at compression face. The strain gauges were installed 100 mm away from column face in one direction. Test results of these measurements are presented in Fig. 13. It is shown that the concrete strain curve for post-tensioned slab without opening S1 was linear while it was non-linear for post-tensioned slab with an opening S2. It can be noticed that as the opening size increased, the concrete strain decreased which reflects less ductile behavior for slabs with opening. It shown also from the two figures that the concrete strain for the post-tensioned slab S1 is more than that for non-prestressed slab S4 due to compressive stress caused by prestressing.

Punching Shear Strength: When the loading was approaching the maximum or ultimate load capacity, the inclined crack has already opened wide and the bottom surface of the slab had already dropped by approximately 5 to 10 mm, giving a certain appearance as if the column had sunk into the bottom of the slab. This drop in the bottom surface of the slab is caused by the occurrence of very wide inclined cracks inside the slab, indicating a punching shear failure. All the tested slabs failed in punching shear mode. The recorded punching shear capacities were the maximum loads reached during testing. These values are shown in Table 1. The slabs without an opening (S1 and S4) had the maximum punching capacity in their series. The lowest capacity in a series is found for slabs with the largest opening size (S3 and S5).

Punching Shear Design: The punching shear strength of a prestressed concrete slab is obtained by calculating a nominal shear stress on a critical shear perimeter at a distance away from the column face. Different codes of practice recommend different equations for punching shear strength. That is, the treatment of prestressing effect, location of critical shear perimeter and tension reinforcement by one code can be quite different from another code.

To treat prestressing effect, the ACI [1] 318-08, CSA [2] A23.3-04 and ECP [3] -07 consider the prestressing force in term of pre-compression stress ($f_{p.c}$) in addition to the vertical component of the prestressing force (V_p). In the BS 8110-97 and CEB-FIP-90, treating the prestressing effect is completely different. The cross-sectional area of the tendons can be replaced by an equivalent area of ordinary reinforcing steel. Then the equivalent reinforcement area is substituted into the relevant expression for the shear strength of an ordinary reinforced concrete slab. The ACI [1], CSA [2] and ECP [3] consider the shear perimeter to be located at 0.5*d* away (d is the effective depth of slab) from the column face whereas BS [4] take it to be at 1.5*d* away and CEB [5] take it to be at 2daway. BS [4] and CEB [5] neglect the effect of an opening that is located farther than 6*d* from the column face while the ACI [1] and CSA [2] neglect such an opening only if it is located farther than 10*d*.

ACI 318-08 [1]: The ACI [1] code recommends that the punching shear strength around interior column in two-way prestressed slabs without shear reinforcement, to be conservatively predicted by:

$$V_c = (\beta_p \sqrt{f_c'} + 0.3 f_{p.c}) b_o d + V_p \quad (1)$$

The punching shear strength of non-prestressed slabs without shear reinforcement can be determined from the lowest of the following expressions:

$$V_c = 0.33\sqrt{f_c'} b_o d \quad (2)$$

$$V_c = 0.17\left(1 + \frac{2}{\beta}\right)\sqrt{f_c'} b_o d \quad (3)$$

$$V_c = 0.083\left(\frac{\alpha_s d}{b_o} + 2\right)\sqrt{f_c'} b_o d \quad (4)$$

Where β_p is the smaller of 0.29 or $0.083(\alpha_S d / b_O + 1.5)$, d equals the distance from extreme tension fiber to centroid of tension reinforcement = 0.8h,$f_{p.c}$ equals the mean effective prestress of concrete, V_p is the vertical component of all effective prestress forces crossing the critical section b_o, β is the ratio of the longer side to the shorter side of the column, α_s is 40 for interior columns,30 for edge columns and 20 for edge columns, $b_o$equals the length of the control perimeter d/2 from support;

ACI [1] limits concrete stresses as follows

f'_c = 35 MPa, 0.86 = $f_{p.c}$ = 3.5 MPa

From Equations (1) to (4) above, it is clear that the ACI 318-08 method ignores the influence of flexural reinforcement on the punching shear capacity. When an opening in the slab is situated at a distance less than 10 times the slab thickness to the column or loaded area, the ACI [1] 318-08 method recommends a reduction in the critical shear perimeter by neglecting that part of the perimeter that is bounded by the projection lines originating from column center to the edges of the opening.

CSA [2] -A23.3-04: According to CSA [2]-A23.3-04, the punching shear strength of post-tensioned slabs without shear reinforcement can be determined from the following equation:

$$V_c = \beta_p \lambda \sqrt{f_c'}\left(\sqrt{1 + \frac{f_{pc}}{0.33\lambda\sqrt{f_c'}}}\right) b_o d + V_p \quad (5)$$

The punching shear strength of non-prestressed slabs without shear reinforcement can be determined from the lowest of the following expressions:

$$V_c = 0.38\sqrt{f_c'}\,b_o d \quad (6)$$

$$V_c = 0.19\left(1+\frac{2}{\beta}\right)\sqrt{f_c'}\,b_o d \quad (7)$$

$$V_c = \left(\frac{\alpha_s d}{b_o}+0.19\right)\sqrt{f_c'}\,b_o d \quad (8)$$

Where β_p is the smaller of 0.33 or $(\alpha_s d/b_o + 0.15)$, α_s is 4 for interior columns, 3 for edge columns and 2 for edge columns and the other factors are same as that in ACI [1] code. The opening in CSA [2] is treated same as that in ACI [1] code.

ECP [3] -07: The Egyptian code ECP [3]-07 calculates the punching shear strength of post-tensioned slabs without shear reinforcement using Eq. (9)

$$V_c = (0.27\sqrt{f_{cu}} + 0.3 f_{p.c})\,b_o d + V_p \quad (9)$$

The punching shear strength of non-prestressed slabs without shear reinforcement can be determined from the lowest of the following expressions:

$$V_c = 0.316\sqrt{f_{cu}}\,b_o d \quad (10)$$

$$V_c = 0.316\left(0.5+\frac{a}{b}\right)\sqrt{f_{cu}}\,b_o d \quad (11)$$

$$V_c = 0.8\left(\frac{\alpha d}{b_o}+0.2\right)\sqrt{f_{cu}}\,b_o d \quad (12)$$

Where a is the shorter side length of the column, b is the longer side length of the column, α_s is 4 for interior columns, 3 for edge columns and 2 for edge columns and the other factors are same as that in ACI [1] code. The opening in ECP[3] is treated same as that in ACI[1] and codes.

BS [4] 8110-97: In BS [4] 8110-97, the punching shear strength of post-tensioned and non-prestressed slabs without shear reinforcement is given by:

$$V_c = 0.79\left(\frac{100A_s}{bd}\right)^{\frac{1}{3}}\left(\frac{400}{d}\right)^{\frac{1}{4}}\left(\frac{f_{cu}}{25}\right)^{\frac{1}{3}} b_o d \quad (13)$$

Where $(A_s/b_o d)$ is the flexural reinforcement plus the tendons equivalent reinforcement ratio, (400/d) is the size effect factor which should not be taken less than 1.0, f_{cu} should not be taken greater than 40 MPa, b_o is the effective shear perimeter. BS [4] 8110 uses a shear perimeter at 1.5d away from the column. For slabs with an opening located within a distance of 6d from the column, BS [4] 8110 considers the part of the perimeter enclosed by the radial projections from the centroid of the column to the opening to be ineffective.

Table 2: Statistical analysis of the predicated values.

	P-test / P-code				
Slab	ACI	CSA	ECP	BS	CEB
S1	2.04	1.70	1.98	1.22	1.00
S2	2.12	1.77	2.06	1.27	1.05
S3	2.22	1.85	2.15	1.28	1.06
S4	1.74	1.52	1.63	1.10	1.20
S5	1.51	1.31	1.41	0.98	1.07
Average	1.93	1.63	1.85	1.17	1.08
S.O.D	0.29	0.22	0.31	0.13	0.07
C.O.V	0.15	0.13	0.17	0.11	0.07

Table 3: Effect of openings and prestressing on measured slab capacities and on the ACI, CSA, ECP, BS and CEB codes predicted values.

		Comparison Between Slab Results					
Effect	Slab	Test	ACI	CSA	ECP	BS	CEB
Opening	S1/S2	1.18	1.23	1.23	1.23	1.24	1.24
Opening	S1/S3	1.53	1.66	1.66	1.66	1.61	1.61
Prestressing	S1/S4	1.04	0.89	0.93	0.86	0.94	1.24
Prestressing	S2/S5	1.22	0.87	0.90	0.83	0.94	1.24
Opening	S4/S5	1.39	1.20	1.20	1.20	1.23	1.24

CEB [5] -FIP-90: According to CEB [5]-FIP-90 code, the punching shear strength of post-tensioned and non-prestressed slabs without shear reinforcement is given by:

$$V_c = 0.12\xi\left(100\rho f_{ck}\right)^{1/3} b_o d \quad (15)$$

where

$$\xi = 1+\sqrt{\frac{200}{d}} \quad (16)$$

The reinforcement ratio (ρ) may be calculated as the average for two orthogonal directions. In each direction the effective width in the calculation of ρ is equal to the side dimension of the column plus 3d to the either side of it.

Analysis of Test Results: All test slabs failed in punching shear. Table 2 demonstrates the ultimate shear capacities predicted by ACI[1], CSA[2], ECP[3], BS[4] and CEB[5] codes of practice. A summary of the effect of openings and prestressing on the punching shear strength is shown in Table 3. The test results compared with the results calculated by each code are shown in Fig. 14.

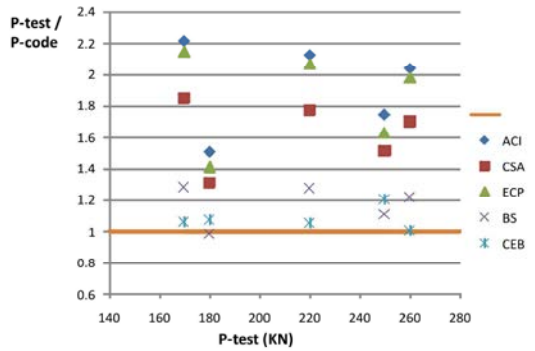

Fig. 14: Ratios of P-test / P-code.

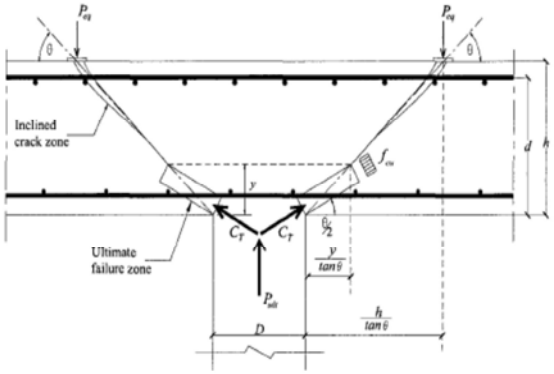

Fig. 15: Strut-and-tie model (Emad Raouf, 2010)

Effect of Openings: According to both experimental and code results, the relationship between the punching effective perimeter and the ultimate punching shear strength was almost linear for post-tensioned slabs and non-prestressed slabs with both small and large openings, The experimental results show good agreement with all code results in estimating the effect of opening on punching shear strength of post-tensioned slabs.

Effect of Prestressing: According to code results, the effect of prestressing was linear for slabs with and without openings, but experimental results show that the effect of prestressing was higher for slabs with openings than slabs without openings. The CEB code shows a good agreement with test results for the slab with opening but for the slab without opening, there is a difference in the results. The experimental results do not show good agreement with the other codes in estimating the effect of prestressing on the punching shear strength for slabs without openings and slabs with openings.

Strut-and-Tie Model Proposed by Rizk [6]: As can be seen in later sections of this paper, the current code equations are conservative, yet the scatter of the predictions showed that improvement could be made. The strut-and-tie model proposed by Rizk [6] for calculating the punching shear strength of non-prestressed slabs, has been used to model the punching shear behaviour of the present post-tensioned slabs. This model provides a quick and simple approach to punching shear behavior. It is applicable for both prestressed and non-prestressed concrete slabs under symmetric loading. The proposed strut-and-tie model presented as follows had been checked against the current experimental data and was found to be more accurate than code formulas except CEB.

$$P_{ult} = \pi\left(D + \frac{2y}{\tan\theta}\right)\frac{y\sin\theta/2}{\sin\theta} f_{c2,\max}\left(\frac{l_{ch}}{h}\right)^{0.33}\sin\theta/2 \quad (17)$$

Where D is column diameter (a square column can be replaced in the equation by an equivalent circular column with the same perimeter i.e. $D = 4C/\pi$ where C is the square column side length), θ is angle of inclination and taken as 26 degrees for non-prestressed slabs and 32 degrees for post-tensioned slabs according to the present experimental results, l_{ch} equals 500 if $f'_c < 40$ Mpa and 250 if $f'_c > 40$ MPa and h is the slab thickness as shown in Fig. 15

$$f_{c2,\max} = \frac{\lambda\phi_c f_c^{'}}{0.8 + 170\varepsilon_1} \le \phi_c f_c^{'} \quad (18)$$

$$y = \frac{A_s f_y}{0.85 f_c^{'} b} \text{ (For non-prestressed slabs)} \quad (19)$$

$$y = \frac{A_s f_y + A_{ps} f_{ps}}{0.85 f_c^{'} b} \text{ (For prestressed slabs)} \quad (20)$$

Recent Researches Data: To provide an adequate basis for comparing test data with the predictions of ACI [1] and ECP [3] equations, the results of the present test which was described previously have been combined with others available in the literature. All of the results considered are for punching failures of post-tensioned slabs with bonded or unbounded tendons and bonded deformed reinforcing bars with fy= 600 MPa. The bars were uniformly spaced across the full widths of the test slabs. The present and recent research data are shown in Table 4.

Analysis of Test Results: The results of the analysis for individual tests are listed in Table 4. The values of V_p have been calculated from the tendon forces at failure,

Table 4 : Recent and present researches data.

Slab	Support size mm	f'_c MPa	f_{pc} MPa	V^p kN	h mm	d mm	ρ%	V_u kN
			Present work					
S1	100 square	30.1	2.03	0.0	120	80	1.40	260.0
S2	100 square	29.6	2.01	0.0	120	80	1.40	220.0
S3	100 square	29.6	1.65	0.0	120	80	1.40	170.0
			Mostafa Saleh					
SHP1	100 square	65.5	2.48	0.0	120	80	1.40	337.0
SHP2	100 square	67.0	2.39	0.0	120	80	1.40	431.0
SHP3	100 square	67.0	2.39	0.0	120	80	1.40	381.0
			Silva					
A1	100 square	37.8	3.31	9.0	125	102	0.62	380.0
A2	100 square	37.8	2.14	10.0	125	108	0.47	315.0
A3	100 square	37.8	3.16	0.0	125	102	0.62	352.7
A4	100 square	37.8	1.98	0.0	125	103	0.51	321.0
B1	200 square	40.1	3.39	32.4	125	108	0.60	582.5
B2	200 square	40.1	2.23	29.9	125	105	0.48	488.0
B3	200 square	40.1	3.12	12.6	125	102	0.63	519.8
B4	200 square	40.1	2.16	12.5	125	100	0.50	458.8
C1	300 square	41.6	3.33	40.5	125	105	0.61	720.0
C2	300 square	41.6	2.26	35.4	125	100	0.50	556.7
C3	300 square	41.6	3.48	17.7	125	100	0.64	636.6
C4	300 square	41.6	2.31	15.4	125	98	0.52	497.1
D1	200 square	44.1	3.34	10.0	125	99	0.68	497.1
D2	200 square	44.1	2.23	12.1	125	101	0.50	385.2
D3	200 square	44.1	2.27	0.0	125	100	0.51	395.2
			August 20, 2014					
D4	300 square	44.1	2.22	39.9	125	106	0.48	531.5
			Correa					
LP2	150 square	52.4	2.19	0.0	130	104	1.17	355.0
LP3	150 square	52.4	4.28	0.0	130	104	1.17	415.0
LP4	150 square	50.7	0.80	7.6	130	104	1.17	390.0
LP5	150 square	50.7	1.33	13.0	130	104	1.17	475.0
LP6	150 square	52.4	1.76	11.0	130	104	1.17	437.0
			Kordino and Nolting					
V1	f200	33.6	1.70	65.7	150	124	0.62	450.0
V2	f200	36.0	1.66	60.6	150	123	0.90	525.0
V3	f200	36.0	3.09	115.6	150	122	0.62	570.0
V6	f200	30.4	1.77	0.0	150	120	0.62	375.0
V7	f200	31.2	1.77	67.5	150	124	0.62	475.0
V8	f200	35.2	1.77	70.3	150	124	0.62	518.0
			Hassanzadah					
A1	f250	31.0	2.79	41.6	220	150	0.18	668.0
A2	f250	28.7	2.74	0.0	220	146	0.18	564.0
B2	f250	43.8	2.12	0.0	220	176	0.29	827.0
B3	f250	41.1	2.21	53.5	220	190	0.29	1113.0
B4	f250	43.2	1.99	0.0	220	190	0.29	952.0
			Shehata					
SP1	150 square	36.5	3.94	18.5	175	140	0.27	988.0
SP2	150 square	41.7	4.81	21.0	175	140	0.27	884.0
SP3	150 square	40.9	3.28	0.0	175	140	0.27	780.0
SP4	150 square	42.5	3.50	0.0	175	140	0.27	728.0
Melges								
M4	180 square	51.90	1.95	0.00	160	128	0.92	773.0

Table 5: Ultimate load predictions with the proposed strut-and-tie model.

Slab	θ	y mm	l_{ch}	b_o mm	$f_{c2,max}$ MPa	P_{STM} kN	P_{test} kN	P_{test} / P_{STM}
S1	32.0	46.5	500.0	867.5	26.4	245.4	260.0	1.06
S2	32.0	47.2	500.0	725.0	26.0	205.1	220.0	1.07
S3	32.0	47.2	500.0	567.0	26.0	160.4	170.0	1.06
S4	26.0	40.0	500.0	915.4	31.1	211.4	250.0	1.18
S5	26.0	40.0	500.0	733.0	31.1	169.3	180.0	1.06
--	--	--	--	--	--	Average	1.09	
--	--	--	--	--	--	S.O.D	0.05	
--	--	--	--	--	--	C.O.V	0.05	

Table 6: Estimated punching shear capacities using the proposed critical perimeter locations according to ECP.

	ECP (0.5d)		(0.7d)		(0.75d)		(0.8d)		(0.9d)		Proposed (d)	
Slab	V_c kN	V_u/V_c	V_c kN	V_u/V_c	V_c kN	V_u/V_c	V_c kN	V_u/V_c	V_c kN	V_u/V_c	V_c kN	V_u/V_c
Present work												
S1	131	1.98	155	1.68	161	1.62	167	1.56	178	1.46	190	1.37
S2	101	2.17	126	1.74	129	1.70	134	1.64	143	1.53	153	1.44
S3	79	2.15	90	1.88	95	1.79	98	1.73	105	1.62	112	1.52
Mostafa Saleh												
SHP1	185	1.82	218	1.55	226	1.49	234	1.44	251	1.34	267	1.26
SHP2	185	2.33	218	1.98	226	1.91	234	1.84	251	1.72	267	1.61
SHP3	185	2.06	218	1.75	226	1.68	234	1.63	251	1.52	267	1.43
Silva												
A1	244	1.56	291	1.30	303	1.25	315	1.21	339	1.12	362	1.05
	ECP (0.5d)		(0.7d)		(0.75d)		(0.8d)		(0.9d)		Proposed (d)	
Slab	V_c kN	V_u/V_c	V_c kN	V_u/V_c	V_c kN	V_u/V_c	V_c kN	V_u/V_c	V_c kN	V_u/V_c	V_c kN	V_u/V_c
						Silva						
A2	234	1.34	281	1.12	293	1.08	304	1.03	328	0.96	351	0.90
A3	231	1.53	278	1.27	289	1.22	301	1.17	324	1.09	348	1.01
A4	205	1.57	246	1.30	257	1.25	267	1.20	288	1.11	309	1.04
B1	422	1.38	477	1.22	490	1.19	504	1.16	531	1.10	559	1.04
B2	360	1.35	406	1.20	417	1.17	429	1.14	452	1.08	474	1.03
B3	363	1.43	411	1.27	423	1.23	435	1.20	458	1.13	482	1.08
B4	320	1.44	361	1.27	371	1.24	381	1.20	402	1.14	422	1.09
C1	542	1.33	594	1.21	607	1.19	620	1.16	646	1.12	672	1.07
C2	455	1.22	497	1.12	508	1.10	518	1.07	539	1.03	560	0.99
C3	496	1.28	544	1.17	556	1.14	568	1.12	592	1.08	616	1.03
C4	427	1.16	468	1.06	478	1.04	488	1.02	508	0.98	529	0.94
D1	366	1.36	413	1.20	425	1.17	437	1.14	460	1.08	484	1.03
D2	337	1.14	381	1.01	392	0.98	403	0.96	425	0.91	446	0.86
D3	322	1.23	365	1.08	376	1.05	387	1.02	408	0.97	430	0.92
D4	500	1.06	548	0.97	560	0.95	572	0.93	596	0.89	620	0.86
Correa												
LP2	300	1.18	350	1.02	362	0.98	374	0.95	399	0.89	423	0.84
LP3	367	1.13	427	0.97	442	0.94	457	0.91	487	0.85	517	0.80
LP4	260	1.50	301	1.29	312	1.25	322	1.21	343	1.14	363	1.07
LP5	282	1.68	326	1.46	337	1.41	348	1.36	370	1.28	393	1.21
LP6	298	1.47	345	1.27	356	1.23	368	1.19	392	1.12	415	1.05
						Kordino and Nolting						
V1	351	1.28	394	1.14	405	1.11	416	1.08	438	1.03	460	0.98
V2	349	1.51	393	1.34	404	1.30	414	1.27	436	1.20	458	1.15
V3	453	1.26	505	1.13	517	1.10	530	1.08	556	1.03	581	0.98
V6	265	1.42	304	1.23	314	1.19	324	1.16	344	1.09	364	1.03
V7	347	1.37	390	1.22	401	1.19	411	1.15	433	1.10	454	1.05
V8	363	1.43	408	1.27	419	1.24	430	1.20	453	1.14	475	1.09

Table 6: Continue

	ECP (0.5d)		(0.7d)		(0.75d)		(0.8d)		(0.9d)		Proposed (d)	
Slab	V_c kN	V_u/V_c	V_c kN	V_u/V_c	V_c kN	V_u/V_c	V_c kN	V_u/V_c	V_c kN	V_u/V_c	V_c kN	V_u/V_c
						Hassanzadah						
A1	516	1.29	587	1.14	605	1.10	623	1.07	658	1.01	694	0.96
A2	443	1.27	508	1.11	524	1.08	541	1.04	573	0.98	606	0.93
B2	620	1.33	723	1.14	748	1.11	774	1.07	825	1.00	876	0.94
B3	736	1.51	853	1.30	883	1.26	912	1.22	971	1.15	1030	1.08
B4	678	1.41	795	1.20	824	1.16	853	1.12	912	1.04	970	0.98
						Shehata						
SP1	507	1.95	601	1.64	624	1.58	648	1.52	695	1.42	742	1.33
SP2	572	1.55	678	1.30	705	1.25	731	1.21	785	1.13	838	1.06
SP3	473	1.65	565	1.38	588	1.33	610	1.28	656	1.19	702	1.11
SP4	490	1.49	585	1.24	608	1.20	632	1.15	679	1.07	727	1.00
						Melges						
M4	435	1.78	508	1.52	526	1.47	544	1.42	580	1.33	616	1.25
Average	1.47		1.27		1.23		1.19		1.12		1.06	
St. of dev.	0.27		0.22		0.20		0.20		0.18		0.16	
C.O.V.	0.19		0.17		0.17		0.16		0.16		0.16	

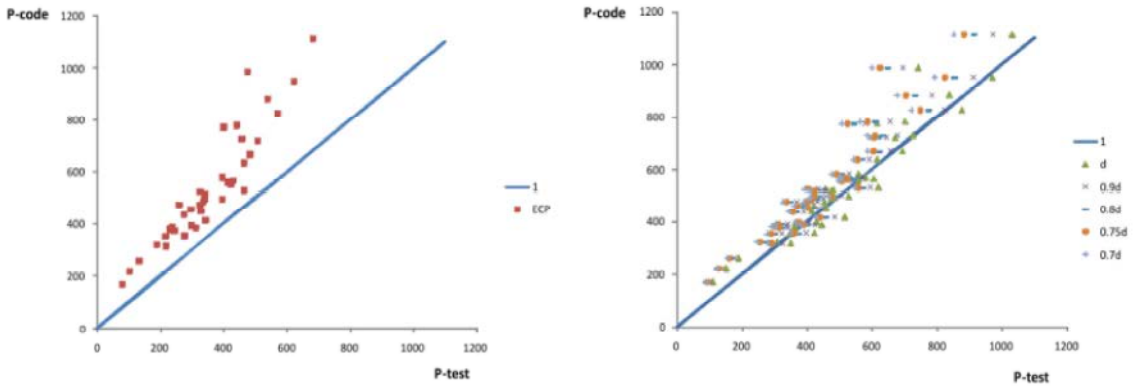

Fig. 16: Comprehensive study for ECP.

which were measured in most cases, but have been estimated for the slabs by Correa [7]. No allowances have been made for the increases of tendon inclination caused by the slabs' deflections. The value of f_{pc} at the start of tests, as listed in Table 5, have been used for determinations of V_u.

Comprehensive Study for Ecp-07: As shown in Fig. 16 the predicted capacities using the ECP [3] equations underestimate all investigated test slab capacities, hence the effect of modifying the critical perimeter location on the predicted capacities is evaluated within this research work. While ECP [3] defines the critical perimeter at d/2 from load face, other codes like BS [4] and CEB [5]-FIP defines it at 1.5d and 2d respectively.

Table 6 shows a study and results for different specimens' results at different critical perimeter at 0.7d, 0.75d, 0.8d, 0.9d and d. The closest capacity predictions resulted when assuming the critical section at 0.7d. This assumption showed the lowest standard of deviation and only 2 specimens were overestimated (5%).

CONCLUSIONS

The size of the opening influences the punching shear capacity of the slab. The relation between the punching effective perimeter and the punching strength is nearly linear for post-tensioned slabs. The angle of inclination for the tested post-tensioned slabs was 32° and the critical perimeter was at 0.85*d* from column face,

while for non-prestressed slabs the angle of inclination was 28° and the critical perimeter was at 0.95*d* from column face. The ACI[1], CSA[2] and ECP[3] codes are very conservative in calculating the punching shear strength for both post-tensioned and non-prestressed slabs. The capacity predictions using the BS [4] code are consistent. A very good agreement between the experimental results and the CEB [5] code predictions is obtained. Increasing the distance of control perimeter from the support from 0.5*d* to 0.75*d* in ACI [1] code equation and from 0.5*d* to 0.70*d* in ECP [3] code equation gives consistence and acceptable results. This conclusion is verified using forty test slabs tested and published by other researchers in addition to the present test slabs. Converting the prestressing steel area to the equivalent reinforcement percentage proposed by BS [4] 8110-97 using the ultimate strength of prestressing steel gives consistent results. CEB [5] -FIP-90 treats the prestressing steel in the same way of BS [4] code but differs in the slab width in which the reinforcement percentage is calculated. Treating the prestressing in ACI[1], CSA[2] and ECP[3] codes are different and give inconsistent results. A strut-and-tie model proposed by Rizk [6] was used for calculating the punching shear strength of the tested slabs. The proposed strut-and-tie model has an average theory/test ratio of 1.09 with a S.D. of 0.05, when compared to the present experimental test results. It can be concluded that the model appears to be equally valid for post-tensioned slabs as well as non-prestressed slabs.

Notations:

b_o = Length of effective punching perimeter.
f'_c = Cylinder strength of concrete.
f_{cu} = Cube strength of concrete.
d = Depth from concrete extreme compressive fiber to centroid of prestressing steel or non-prestressed tensile steel.
f_{pc} = Mean effective prestress of concrete.
V_p = Vertical component of tendon forces near support.
V_u = Experimental punching strength.

REFERENCES

1. ACI Committee 318, 2008. Building Code Requirements for Structural Concrete and Commentary, ACI 318M-08. American Concrete Institute, Michigan, USA.
2. CSA A23.3, 2004. Design of Concrete Structures for Buildings. Canadian Standards Association, Ottawa, Canada.
3. ECP 203, 2007. Egyptian Code of Practice for Design and Construction of Concrete Structures ECP-07, Cairo, Egypt.
4. British Standards Institution. Structural Use of Concrete, Part 1 and Part 2, Code of Practice for Design and Construction BS 8110-97, London, UK.
5. CEB-FIP MC90 Model Code, 1990. Model Code For Concrete Structures. Comintary International du Baton et federation International de la Precontrainte, Lausanne, Switzerland.
6. Rizk, E.R.M., 2010. Structural Behaviour of Thick Concrete Plates. M.Phil. Thesis, University of Newfoundland, July.
7. Corrêa, G.S., 2001. Puncionamentoem Lajes Cogumelo Protendidas com Cabos Não Aderentes (Punching in flat slabs with unbounded prestressed cables). M.Sc. dissertation, Department of Civil and Environmental Engineering, University of Brasília, Brasília, Brazil, pp: 153.